Defense Technical Information Center Compilation Part Notice

ADP013787

TITLE: Photoluminescence Mapping and Angle-Resolved Photoluminescence of MBE-Grown InGaAs/GaAs RC LED and VCSEL Structures

DISTRIBUTION: Approved for public release, distribution unlimited

This paper is part of the following report:

TITLE: THIN SOLID FILMS: An International Journal on the Science and Technology of Condensed Matter Films. Volume 412 Nos. 1-2, June 3, 2002. Proceedings of the Workshop on MBE and VPE Growth, Physics, Technology [4th], Held in Warsaw, Poland, on 24-28 September 2001

To order the complete compilation report, use: ADA412911

The following component part numbers comprise the compilation report:
ADP013771 thru ADP013789

ELSEVIER

Thin Solid Films 412 (2002) 114–121

thin solid films

www.elsevier.com/locate/tsf

Photoluminescence mapping and angle-resolved photoluminescence of MBE-grown InGaAs/GaAs RC LED and VCSEL structures

A. Wójcik, T.J. Ochalski, J. Muszalski*, E. Kowalczyk, K. Goszczyński, M. Bugajski

Institute of Electron Technology, Al. Lotników 32/46, 02-668 Warsaw, Poland

Abstract

In this paper we report a systematic investigation of emission properties of microcavity devices [resonant-cavity light-emitting diodes (RC LEDs) and vertical-cavity surface-emitting lasers (VCSELs)] fabricated from molecular beam epitaxy (MBE)-grown heterostructures. The optimization of such structures requires proper tuning of the wavelength of radiation emitted from the quantum-well active region, the peak reflectivity of Drs and the cavity resonance. We demonstrate results of two techniques used to study InGaAs/GaAs RC LED and VCSEL structures. The first method is spatially resolved photoluminescence, i.e. mapping of the spontaneous emission and the cavity resonance wavelength over the whole epitaxial structure, which allows for precise determination of wavelength tuning of the structure with resonant cavity. On the other hand, it should be borne in mind that the frequency of the cavity resonance depends on the angle of observation. To study this effect we performed angle-resolved emission measurements, which yield information about the directionality of RC LED emission. The results of the study provide a better understanding of the physical processes underlying light generation in microcavity devices. The information provided by both methods is crucial for designing optimum MBE growth processes and for selecting the areas of the wafer from which useful devices can be fabricated. Since the measurements were made at room temperature they are directly applicable to devices.

Keywords: Photoluminescence; Photoluminescence mapping; Angle-resolved photoluminescence; Microcavity; Resonant cavity light emitting diode (RC LED); Vertical cavity surface emitting laser (VCSEL)

1. Introduction

Vertical-cavity surface-emitting laser (VCSEL) and resonant-cavity light-emitting diodes (RC LED) belong to the new generation of semiconductor optoelectronic devices. Such devices benefit from the utilization of specific effects resulting from placing the active structure inside a Fabry–Perot-type microcavity. The main advantage of resonant-cavity LEDs is higher emission intensity, higher spectral purity and more directional emission patterns. In addition, such devices are small in size, which enables single-mode operation with large-modulation bandwidth. Therefore, despite the complicated growth technique, microcavity devices have attracted much attention in recent years [1].

Epitaxial growth of VCSELs and RC LEDs represents possibly the greatest challenge among optical devices. The high degree of complexity of the epitaxial structure (often with more than 100 discrete epitaxial layers, including complex composition and doping schemes), along with the precision and uniformity required, has posed strong limitations on the process and necessitated a massive efforts at characterization to evaluate the structures grown. One of the basic conditions to obtain high quantum efficiency for surface emitter structures is proper tuning of the wavelength of radiation emitted from the active region (quantum well), the peak reflectivity of DBRs and the resonance of the GaAs microcavity (see Fig. 1). The optimum performance of the structure requires simultaneous alignment of all three features. This is the reason why the performance of surface emitters is very sensitive to variations in thickness of the individual layers and their composition.

In this study we mainly concentrated on the emission properties of InGaAs/GaAs RC LEDs, although the methods used are equally applicable to more complicated VCSEL structures. The device structures were grown by molecular beam epitaxy (MBE) using a Riber 32P reactor. Details of the growth can be found in our earlier

*Corresponding author. Tel.: +48-22-5487-920; fax: +48-22-8470-631.

E-mail address: muszal@ite.waw.pl (J. Muszalski).

0040-6090/02/$ - see front matter
PII: S0040-6090(02)00322-X

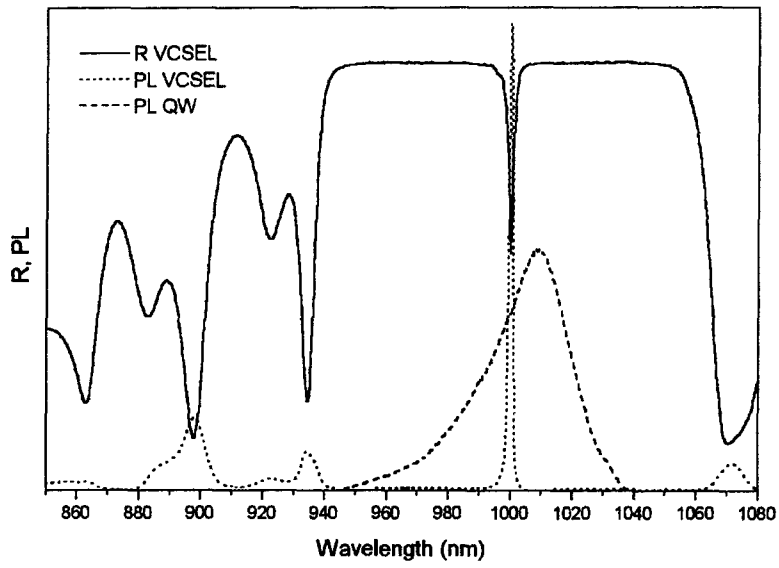

Fig. 1. Reflectance and photoluminescence spectra of surface emitter structure.

paper [2]. This technology allows control of the growth rate of particular layers and their composition with high accuracy (in our case better than 2%). In an MBE reactor, molecular beams hit the center of a rotating sample. However, due to the transversal distribution of the molecular beam intensity, the growth rate is radially non-uniform. This in turn produces a similar inhomogeneity in the layer thickness. This is an inherent property of MBE technology, which cannot be completely eliminated. For typical 2-inch-diameter substrates, the maximal difference in layer thickness over the sample may reach a few percent. Such inhomogeneity of the sample parameters means that proper tuning between the quantum well (QW) emission and the cavity resonance can be achieved only on limited area of the sample (see Fig. 2). In general, the surface emitter structures are very dependent on the capability and limitations of the epitaxial process. Thus, the critical issue is to non-destructively evaluate the wafers grown with respect to the degree of tuning, and select material for further processing. For that purpose we propose fully automated, spatially resolved photoluminescence (PL) mapping and angle-resolved local PL measurements. This high-resolution technique consists of intensity and peak-wavelength mapping over the whole epitaxial wafer and is an extension of previously proposed intensity mapping [3]. The information provided by the spatially resolved PL maps are very useful for determining areas where the cavity resonance and QW emission are aligned to each other. In addition, it should be borne in mind that the frequency of the cavity resonance depends on the angle of observation. This means that emission from surface emitter structures shifts to shorter wavelengths with increasing angle between the direction of observation and the normal to the surface. Therefore, the angle-resolved emission studies, as well as the spatial PL mapping, are important for understanding the emission features of RC LED and VCSEL structures, as well as the RC LED device itself, for which they help in selecting a proper cavity design for high brightness and maximum extraction efficiency of the diodes.

2. Experimental

In this paper we report a systematic investigation of InGaAs/GaAs RC LED structures optimized for emission at 1000 nm. The design, fabrication and basic characteristics of these devices have been previously

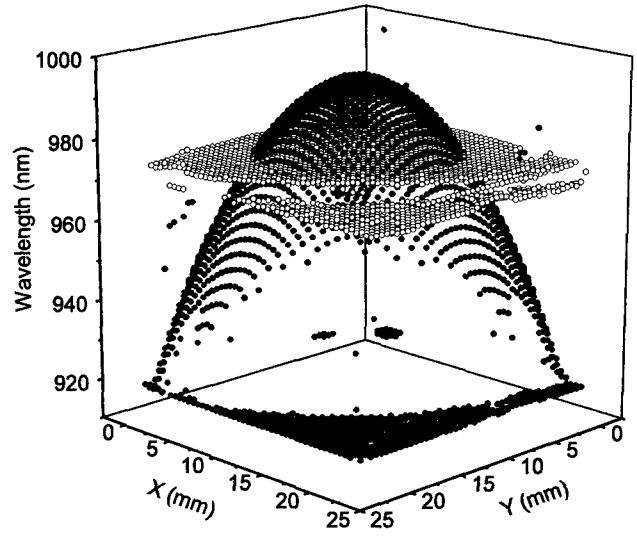

Fig. 2. Typical set of data representing wavelength distribution of PL maximum from QW (*white circles*) and Fabry–Perot microcavity resonance (*black circles*).

described [4]. The RC LEDs utilize the λ-type resonance cavity, constructed normal to the substrate plane by stacking multilayer films, including an active region (consisting of three 80-Å $In_{0.2}Ga_{0.8}As$ quantum wells), a spacer and two dielectric mirrors. Such a structure forms a one-dimensional Fabry–Perot cavity resonator and, due to photon confinement, enhances and concentrates QW emission into a narrow (~1.5 nm half-width), intense line [5].

For the PL measurements we used a tunable titanium–sapphire laser pumped by an ion argon laser. The exciting beam is focused on the sample by special imaging optics, providing a spot diameter of the order of 3 μm. The excitation wavelength of 700 nm at 300 mW of power allows penetration of the multilayer structure deep enough to excite the optically active region, but does not cause heating effects. The scanning module used in spatial PL mapping is based on an *X–Y* piezo-stage combined with mechanical encoders for approximate positioning. The measurement points are nodes of square mesh of constant step, which cover the surface of the sample. A CCD camera records the whole emission spectrum for the structure being investigated for each measurement point at once. The same procedure is then repeated for the next measurement point. However, saving and processing such a huge amount of data is difficult, so each spectrum is numerically processed and only the main signatures of the spectra, such as the wavelength of PL maximum, the half-width and the integrated intensity, are saved on disk. In this way we obtain a set of three characteristic maps from each measurement cycle. The spectral signatures are calculated in real time. The full measurement cycle takes on average from 10 min to few hours, depending on the wafer size, the resolution and the intensity of the signal. The set-up used for angle-resolved photoluminescence studies was analogous to the spatial mapping system. The only difference is in the way the signal is detected, i.e. a fiber-optic cable placed on rotary arm collects the PL signal from a small solid angle for a particular angle of observation, instead of collecting the signal from a large solid angle, as is the case for the CCD camera. The angle-resolved photoluminescence is locally investigated, but due to the fact that the sample is mounted on an *X–Y* stage, the points at which measurements are taken can be precisely identified, and thus the results can be correlated with spatially resolved PL maps.

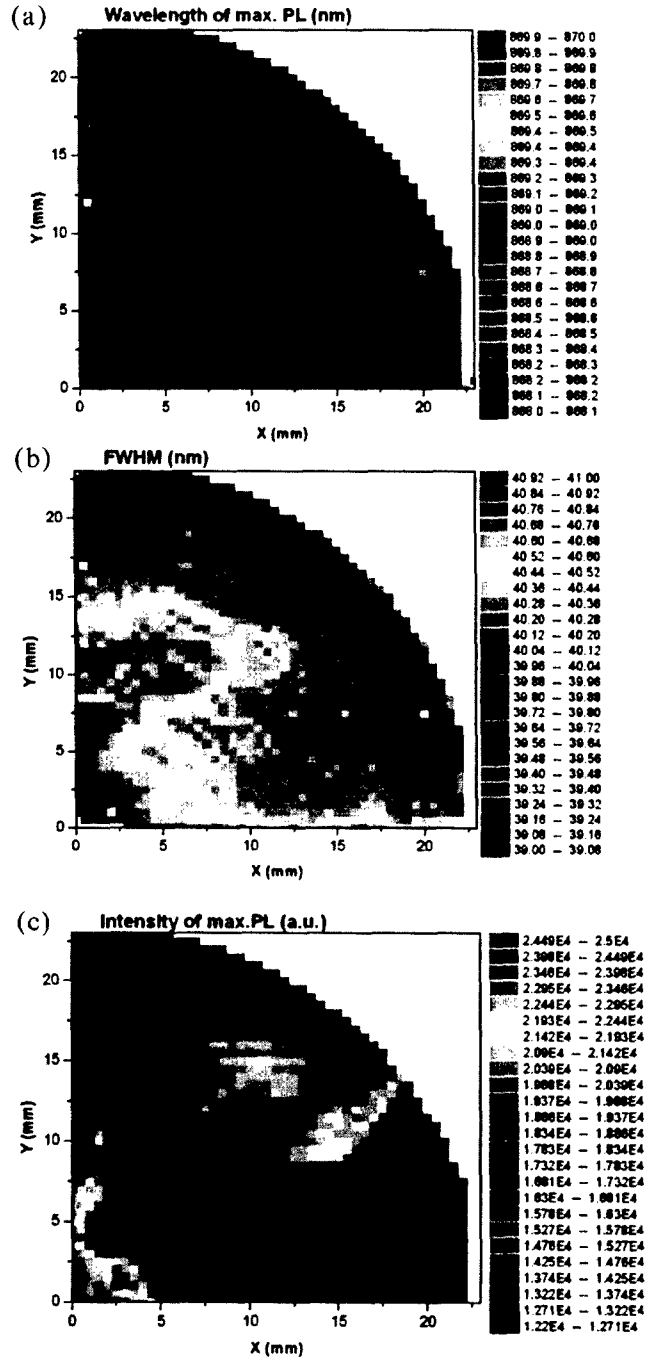

Fig. 3. PL maps of n^+-type GaAs substrates: the distribution of PL maximum wavelength from (a) QW, (b) FWHM and (c) the intensity of the PL signal.

3. Results and discussion

3.1. Spatially resolved PL mapping

Before the final device structures were grown and investigated, photoluminescence measurements were made on substrate wafers and structures containing device-active regions (3×QW) but no DBRs. In both cases the complete set of maps representing characteristic features of the wafers being investigated was recorded. These maps served as a reference when the final RC LED structures were assessed and allowed us to identify the areas of the wafers suitable for making devices. All measurements were made on one-quarter 2-inch wafers. Fig. 3 shows PL maps of the GaAs substrate (i.e. PL peak wavelength, half-width and intensity). The

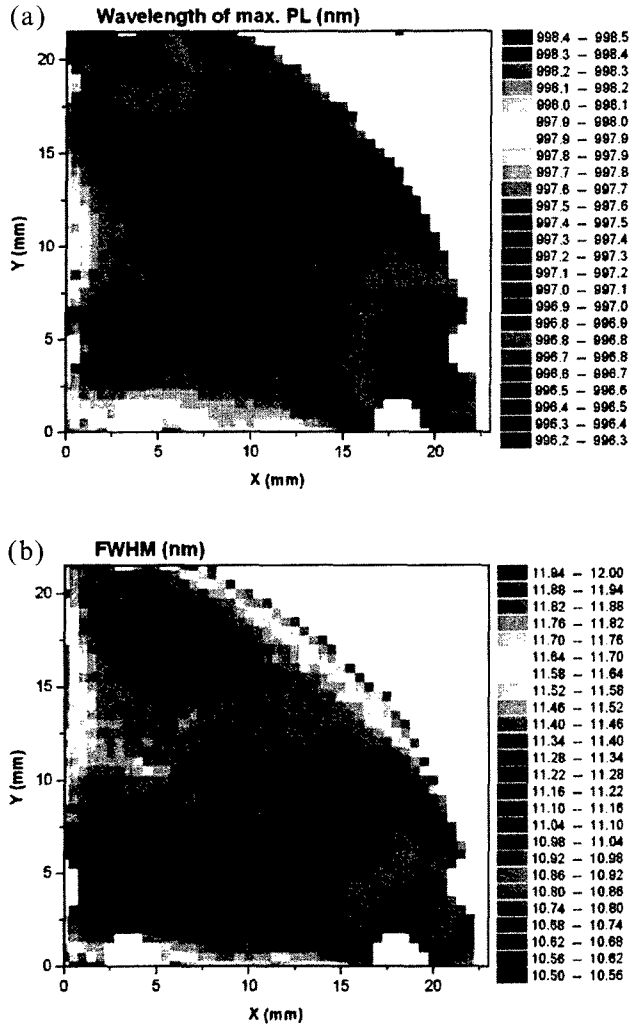

Fig. 4. Set of device active region maps (3×QW InGaAs/GaAs): the distribution of the wavelength of PL emission from (a) QW and (b) FWHM.

peak wavelength variations (see Fig. 3a) over the whole wafer are within 0.5 nm (868.0–8685 nm) with no specific pattern visible, except that the longer peak wavelengths are observed at the outer edges of the wafer. The full width at half-maximum (FWHM) value is also very uniform and equal to approximately 40 nm (Fig. 3b). Slightly higher values of the half-width (up to 41 nm) are observed at the center of the wafer. Finally, the PL intensity distribution is shown in Fig. 3c. It can be correlated with a typical liquid-encapsulated Czochralski (LEC) crystal dislocation distribution. The macroscopic distribution of dislocations over such wafers demonstrates quadruple symmetry predicted theoretically [6,7] and observed experimentally [8]. The variations of the FWHM can be interpreted as resulting from the dislocation-induced strain in the substrate. Nevertheless, all non-uniformities of the PL features observed are small and within acceptable limits for standard GaAs substrates.

The subsequent set of PL maps, shown in Fig. 4, refers to a diode structure without DBRs. The map of maximum PL wavelength (Fig. 4a) and map of FWHM (Fig. 4b) provide information about uniformity of PL features of active region, which consist of three InGaAs quantum wells embedded in GaAs. The emission wavelength distribution is practically constant, because the several-percent change in QW thickness does not have a significant influence on the ground-state exciton energy. The small differences observed in PL wavelength and half-width can be explained as resulting from inhomogeneity of the indium distribution (affecting the QW composition) over the sample. The lower left corner of the wafer emits the longest wavelengths. It corresponds to the highest indium concentration in the quantum wells, i.e. the lowest substrate temperature during growth of the InGaAs layers. The lower right and top left areas emit shorter wavelengths. The center of the sample is characterized by high uniformity of the PL wavelength: the differences observed do not exceed 2 nm. The source of the wavelength variation is the non-uniform temperature distribution over the substrate caused by preferential heat extraction by the substrate holders (note the darker regions at the corners of the wafer). In addition, the map of FWHM confirms the uniformity of emission over the whole wafer (relative changes of FWHM value are lower than 5%).

Fig. 5 shows mapping results for the final device structure. The characteristic circular symmetry of the PL wavelength distribution from the 3×QW active region embedded in the GaAs cavity enclosed by DBRs is evident (see Fig. 5a). The longest PL wavelength (~1000 nm) is observed at the center of the sample, where the thickness of the layers is the highest and the PL wavelength decreases (down to 930 nm) moving towards the edges of the sample. In the case of a λ-type cavity, the peak wavelength of the photoluminescence emerging outside the microcavity is directly related to its thickness. For the range of changes in the emission wavelength observed, the optical thickness of the GaAs microcavity ($n=3.5$) varies from 286 nm at the center to 266 nm at the wafer edges. Although QWs emit at practically a constant wavelength (approx. 997 nm) the emission extracted from the structure is filtered by the Fabry–Perot (F-P) resonance, which is strongly dependent on the optical thickness of the cavity. The PL intensity map is shown in Fig. 5c. The signal is largest in areas where the peak of QW emission matches the resonant cavity wavelength. The best coupling occurs at 975 nm, and the area of the sample for which this condition is nearly satisfied takes the shape of a ring. We can observe that the value of PL intensity is five-fold higher in the 'tuned area' compared to that observed at the center of the sample. The origin of the high-intensity ring can be understood looking at Fig. 2, which shows the wavelength distribution for QW emission and

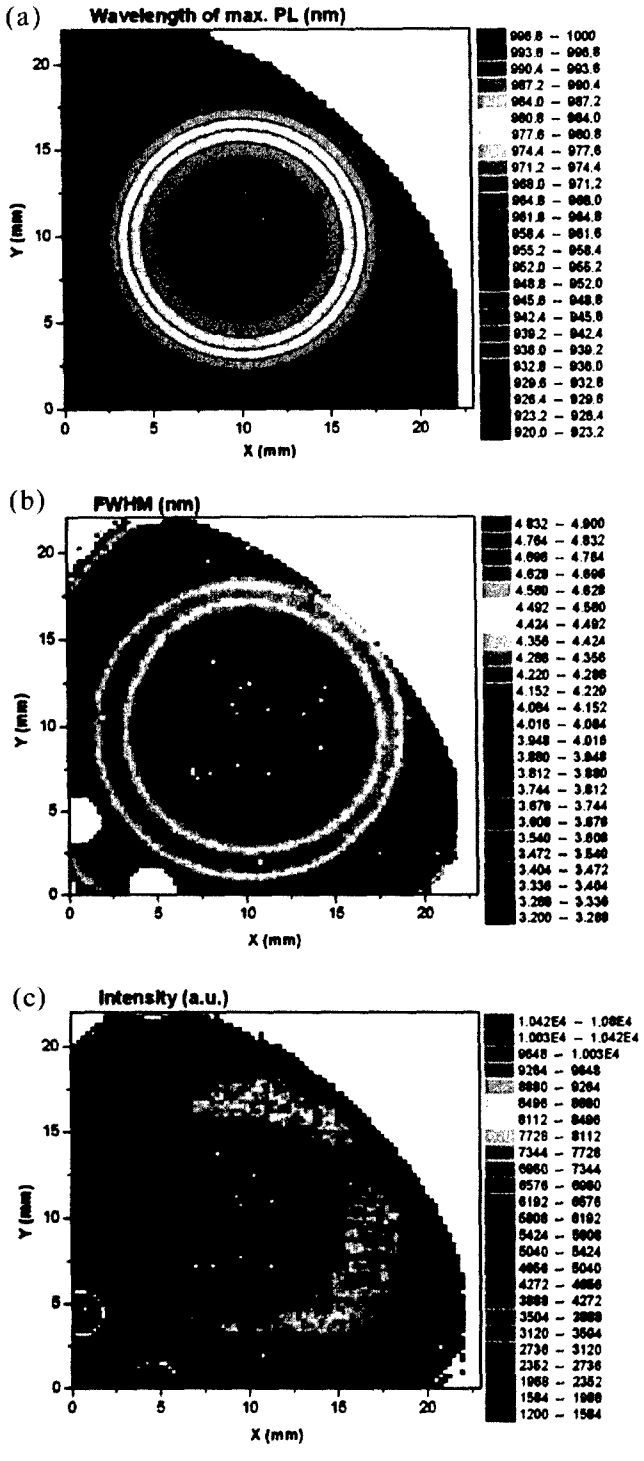

Fig. 5. Maps of characteristic features of RC LED structure: the distribution of PL maximum wavelength from (a) QW, (b) FWHM and (c) the intensity of the PL signal.

that of cavity resonance. In addition, it can be noted that the areas of greatest emission intensity in the final structure overlap with the highest-intensity areas of the substrate; however, emission tuning is still the main factor determining the PL intensity. Finally, Fig. 5b shows a map of FWHM of the structure emission. The values of FWHM are largest in the areas where the QW emission overlaps with the resonant cavity wavelength (4.9 nm), and smallest in the center of the sample (3.2 nm). The distribution of FWHM values also takes a regular ring shape.

In summary, the basic condition to obtain high quantum efficiency for surface emitter structures is proper tuning of the wavelength of radiation emitted from the active region (quantum well) and of the resonance of the GaAs microcavity. The performance of surface emitters is very sensitive to variations in thickness of the individual layers and their composition. PL mapping can be used as the main method to assess the technology and select material meeting the device requirements.

3.2. Angle-resolved photoluminescence

For the purpose of coupling light from an RC LED into a multimode optical fiber, we are only interested in the main emission lobe of the microcavity. Therefore, it is important to obtain high light intensity along the normal direction, where it best couples to the fiber. As has been demonstrated in the previous section, in order to obtain high quantum efficiency of surface emitter structures, the wavelength of radiation emitted from the quantum well must be tuned to the cavity resonance.

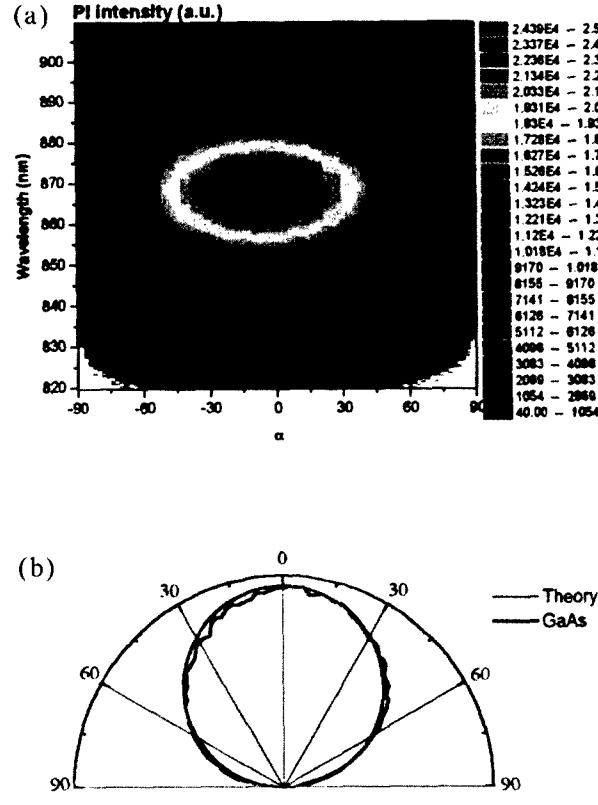

Fig. 6. (a) Angle-resolved map of PL intensity for GaAs substrate and (b) directional characteristics of emission presented in polar coordinates.

On the other hand, it should be borne in mind that the frequency of the cavity resonance depends on the angle of observation. This means that for the cavity, which is positively detuned, i.e. for which cavity resonance occurs at longer wavelength than QW emission, it is possible to enhance the emission by extracting light at a non-zero angle with respect to the normal direction. This occurs, however, at the cost of the directional emission characteristic, which becomes multi-lobed. We now address these issues in some detail. To study the above-mentioned effects, we performed angle-resolved emission measurements, which yield information about the directionality of RC LED emission. As a reference we investigated the angular emission properties of the substrate and the QW active region. Fig. 6a shows an angle-resolved map of the photoluminescence of the GaAs substrate. The horizontal axis represents the angle at which emission is observed (0 refers to normal direction) and the vertical axis represents the wavelength; the tones denote PL intensity. The whole map is characteristic for a particular point on the sample. For bulk material the character of the map does not depend on the position on the sample. In accordance with expectations, the highest intensity of emission occurs at the direction normal to the surface and then decreases

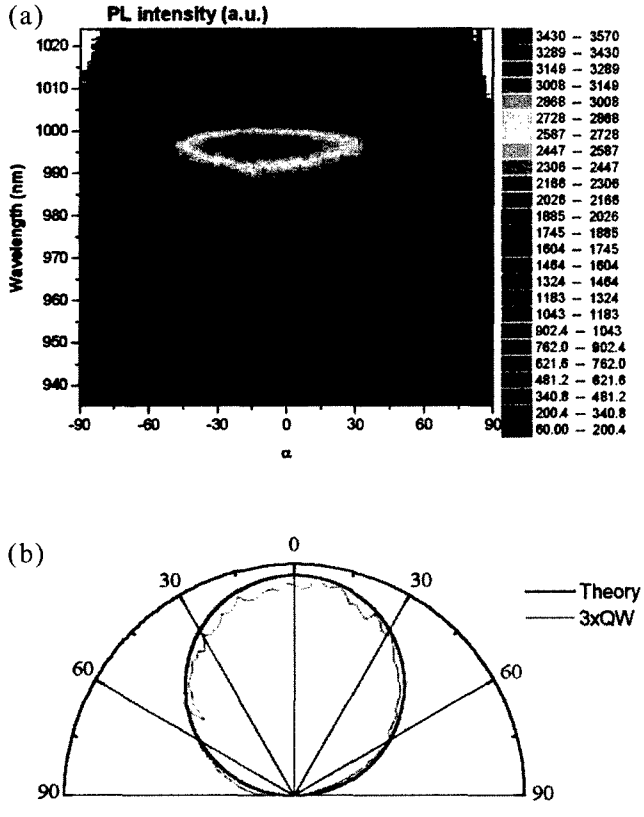

Fig. 7. (a) Angle-resolved map of PL intensity of active region (3×QW) and (b) directional characteristics of emission presented in polar coordinates.

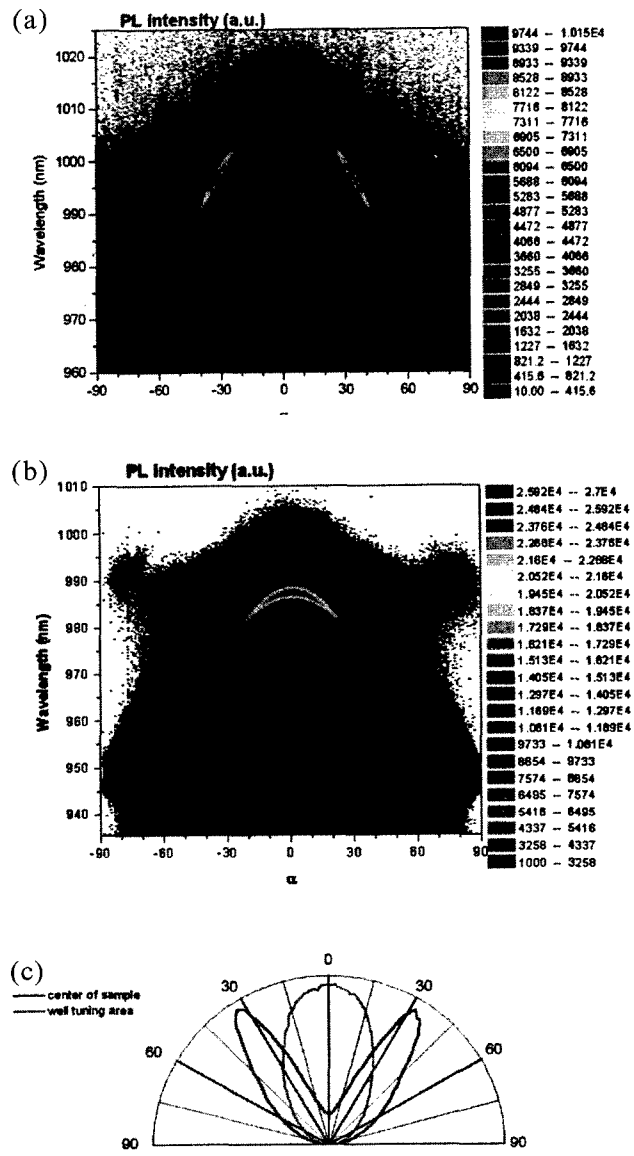

Fig. 8. Angle-resolved spectra of photoluminescence intensity of final RC LED structure: (a) positively detuned and (b) tuned; and (c) directional characteristics of emission presented in polar coordinates.

with angle. Over the whole range of angles, the wavelength of PL maximum equals 870 nm and corresponds to the bandgap energy of GaAs at room temperature. The FWHM of the PL signal is also constant and equal to 40 nm. The integrated PL intensity vs. angle of observation is shown in Fig. 6b. It agrees very well with the theoretical dependence: $I = I_0 \cos(\alpha)$.

The angle-resolved PL measurements of the QW active region demonstrated similar behavior, i.e. there was no difference in the spectra observed at various angles. The map of angle-resolved PL of the QW active region is shown in Fig. 7a. The PL maximum is observed at 998 nm and the FWHM value is equal to 15 nm. The integrated PL intensity vs. angle of observation shown in Fig. 7b obeys the cosine law.

When the QW active region is embedded in the planar microcavity with DBRs, we deal with completely different behavior. In that case not only are the spectral characteristics of emission modified, but we observe also very complex directional features in the spectra. The angular PL maps, shown in Fig. 8, exhibit different features at different positions on the wafer. Their character depends on the tuning between QW emission and the cavity resonance at a given point on the sample. The general feature of angle-resolved PL is its shift to shorter wavelengths with increasing observation angle with respect to the normal direction. The first set of results, shown in Fig. 8a, is characteristic for a positively detuned area located at the center of the wafer (within the high PL intensity ring, cf. Fig. 5c). The second set shows features typical for tuned areas, i.e. from the high PL intensity ring (see Fig. 8b). At the geometrical center of the sample the cavity is the thickest, and the resonance occurs at longer wavelength than QW emission, i.e. at 1010 compared to 995 nm. Consequently, the PL intensity in the direction perpendicular to the surface is rather low. With increasing angle of observation the cavity resonance moves towards shorter wavelengths and PL intensity grows, reaching a maximum at 34°, after which it decreases again. This behavior is shown in Fig. 8a. The corresponding angular distribution of emission intensity is shown in Fig. 8c. A full spatial distribution of emitted radiation can be obtained by rotating the characteristics around the normal to the surface. If we observe the area of the sample which is tuned (see Fig. 8b), the angular characteristics show the same behavior in terms of wavelength shift. However, in this case the maximum PL intensity is observed in the direction perpendicular to the sample and the integrated intensity characteristic is single-lobed (Fig. 8c). In addition, the angular characteristics of the integrated intensity are more directional (much narrower) than in the case of emission from planar sources without a microcavity. This is an important feature and a clear advantage when coupling into the fiber is considered. Thus, for tuned microresonators we obtain spectrally concentrated, narrow emission with the majority of photons emitted in the direction perpendicular to the surface of the resonator, which may also be wavelength-shifted by changing the angle of observation. Such light sources can find interesting applications in molecular spectroscopy, gas analysis and detection systems.

4. Conclusions

We report results of spatially resolved PL mapping and angle-resolved PL measurements of surface emitter structures (RC LEDs and VCSELs). We have found that a small non-uniformity in the radial thickness of the layers, inherent in MBE technology, does not practically influence the spectral position of PL emission from QWs; on the other hand, it is high enough to substantially influence the cavity resonance wavelength. This makes it difficult to grow surface emitter structures that are perfectly tuned over large areas. Results of PL investigations confirm that the emission intensity from RC LED structures is highest in areas of sample where the optical thickness of the microcavity is equal to the wavelength of emission from the QW. The high-resolution mapping method developed allows for identification of areas of the wafer that meet design criteria and can be used for device fabrication. The technique of global spatially resolved PL mapping has been found very useful in technological practice; however, the local measurement technique—angle-resolved PL—is indispensable for correct description of the emission characteristics of microcavity devices. The optical studies reported in this paper have strict connection with MBE technology and should be useful for designing an optimum growth process, and since the measurements were made at room temperature they are directly applicable to the devices. The results of the paper also contribute to better understanding of light emission from optical microresonators, where spatial dimensions are of the order of the wavelength of light. Spontaneous emission, which has long been believed to be uncontrollable, is strongly modified. The changes include not only the emission rate, but also the spectral purity and emission pattern. The last two parameters were studied in considerable detail in the present paper. These changes can be employed to make more efficient and brighter optoelectronic semiconductor devices.

Acknowledgments

This work has been partly supported by the State Committee for Scientific Research (Poland), under Contract No 8T11B 020 18

References

[1] C. Wilmsen, H. Temkin, L.A. Coldren (Eds.), Vertical-Cavity Surface-Emitting Lasers: Design, Fabrication, Characterization and Applications, Cambridge University Press, 1999.

[2] K. Reginski, J. Muszalski, M. Bugajski, T. Ochalski, J.M. Kubica, M. Zbroszczyk, J. Katcki, J. Ratajczak, Thin Solid Films 367 (2000) 290.

[3] M. Bugajski, P. Edelman, M. Wesolowski, J. Ornoch, W. Lewandowski, K. Kucharski, Mater. Sci. Eng. B 20 (1993) 186.

[4] J. Muszalski, T. Ochalski, E. Kowalczyk, A. Wójcik, H. Wrzesinska, B. Mroziewicz, M. Bugajski, 9th International

Symposium on Nanostructures: Physics and Technology, St. Petersburg, Russia, 18–22 June, 2001, p. 171.
[5] T. Ochalski, J. Muszalski, M. Zbroszczyk, J. Kubica, K. Reginski, J. Katcki, M. Bugajski, in: M.L. Sadowski, et al. (Eds.), Optical Properties of Semiconductor Nanostructures, NATO Science Series 3, High Technology, vol. 81, Kluwer Academic Publishing, 2000, p. 201.
[6] A.S. Jordan, R. Caruso, A.R. von Neida, J.W. Nielsen, J. Appl. Phys. 52 (1981) 3331.
[7] A.S. Jordan, A.R. von Neida, R. Caruso, J. Cryst. Growth 70 (1988) 555.
[8] M. Bugajski, P. Edelman, J. Ornoch, Acta Phys. Pol. A 77 (1989) 145.